LETTER TO THE EDITOR

Geometric integration for a two-spin system

R I McLachlan and D R J O'Neale

Institute of Fundamental Sciences, Massey University, Private Bag 11222, Palmerston North, New Zealand

E-mail: r.mclachlan@massey.ac.nz

Abstract
Systems consisting of two interacting magnetic moments, or spins, in an applied magnetic field play a role in the study of quantum chaos where they are used as a classical analogue of a quantum spin system. The equations of motion for such systems are particularly amenable to solution via a geometric integrator constructed by splitting the Hamiltonian into integrable pieces. Such methods have the advantage of restricting numerical solutions to the correct manifold and respecting various geometric properties of the system. Some of these properties, such as approximate conservation of total energy, are important when producing Poincaré surfaces of section (PSSs) which are used to study the onset of chaos in the classical system. The choice of coordinate system for the equations of motion is also important with some choices leading to coordinate singularities. We compare PSSs obtained via a generalized 'leapfrog' integrator with those from a classical 'black-box' Runge–Kutta integrator. The effects of the coordinate singularity on the accuracy and the energy of the solution is also investigated.

PACS numbers: 75.10.Dg, 05.45.Pq
Mathematics Subject Classification: 37M15, 65P10, 65D30

The model Hamiltonian for a system of two interacting magnetic moments in an applied magnetic field can be given by

$$H(\vec{S}_1, \vec{S}_2) = -J(S_{1x}S_{2x} + S_{1y}S_{2y}) + \lambda(S_{1x} + S_{2x}), \tag{1}$$

where $\vec{S}_l = [S_{lx}, S_{ly}, S_{lz}]^T$, $l = 1, 2$ are the angular momentum vectors in $\mathbb{R}^3$. The coupling strength is $J \in \mathbb{R}$ and the applied magnetic field strength is $\lambda \in \mathbb{R}$. Such systems can be viewed as the classical analogue of quantum spin systems and play a role in the investigation of quantum chaos where they are used to study the correspondence between classical and quantum dynamical systems [1–3]. In Cartesian coordinates the equations of motion for the system (1) are given by

$$\frac{d\vec{S}_l}{dt} = -\vec{S}_l \times \frac{\partial H}{\partial \vec{S}_l} = [S_{lx}, S_{ly}, S_{lz}]^T \times [JS_{mx} - \lambda, JS_{my}, 0]^T, \qquad l \neq m. \tag{2}$$

This is a Lie–Poisson system with the generalized Poisson bracket $\{F, G\}(\vec{S}) = \nabla F(\vec{S})^T \mathcal{J}(\vec{S}) \nabla G(\vec{S})$, $\vec{S} = \left[\vec{S}_1^{\,T}, \vec{S}_2^{\,T} \right]^T$, where $\mathcal{J}(\vec{S})$ depends linearly on $\vec{S}$, namely,

$$\mathcal{J}(\vec{S}) = \begin{bmatrix} \text{skew}(\vec{S}_1) & 0 \\ 0 & \text{skew}(\vec{S}_2) \end{bmatrix}.$$

The equations of motion (2) can be expressed compactly as $\frac{d}{dt} \vec{S} = X_H := \mathcal{J}(\vec{S}) \nabla H(\vec{S})$. The system has $\frac{1}{2} \|\vec{S}_l\|^2$ as casimirs; i.e., $\left\{ \frac{1}{2} \|\vec{S}_l\|^2, G(\vec{S}) \right\} = 0$ for all G.

When either J or λ is zero the system is integrable. For both J and λ non-zero the system appears to be non-integrable, with chaotic trajectories appearing in the Poincaré sections.

Writing $\vec{S}_l = [\sin \theta_l \cos \phi_l, \sin \theta_l \sin \phi_l, \cos \theta_l]$ (i.e. $\|\vec{S}_l\| = 1$) allows us to give a local change of coordinates to canonical form with $p_l = \cos \theta_l$ and $q_l = \phi_l$. The corresponding equations of motion then have the usual form $\frac{d}{dt} [q, p]^T = \mathcal{J} \nabla H(q, p)$, $\mathcal{J} = \begin{bmatrix} 0 & I \\ -I & 0 \end{bmatrix}$. When written in terms of ϕ_l and θ_l these are

$$\dot{\phi}_l = J \cos(\phi_l - \phi_m) \cot \theta_l \sin \theta_m - \lambda \cot \theta_l \cos \phi_l \qquad (3)$$

$$\dot{\theta}_l = -J(-1)^l \sin \theta_m \sin(\phi_l - \phi_m) - \lambda \sin \phi_l. \qquad (4)$$

In these coordinates $\dot{\phi}_l$ is singular at $\theta_l = 0$.

The equations of motion (3) and (4) have the advantage that solutions of the equations are automatically constrained to the correct symplectic manifold (the Cartesian product of two unit spheres). The price of this is that the singularities in (3) can cause problems for numerical integrators when the solution passes close to the north or south pole of the sphere.

The Lie–Poisson system given by (2) is amenable to solution via a geometric integrator consisting of the composition of three planar rotations [4–8]. This is similar to the well-studied case of (geometric numerical) integration of the free rigid-body [9–12]. Possible advantages of such a treatment are as follows:

- Using Cartesian coordinates instead of the spherical coordinates in (3) and (4) avoids the problem of singularities (at $\theta_i = 0 \mod \pi$).
- The integrator preserves the Hamiltonian structure of the system, (i.e. is symplectic), and hence, approximately conserves the total energy. This is important for PSSs where solutions are computed on a constant energy manifold.
- The geometric integrator can be implemented very cheaply. The trigonometric functions in the rotation matrices can be replaced with a suitable approximation to further reduce the cost of the method.
- The rotation matrices used for the geometric integrator all have a determinant of one. This conserves the casimirs $\frac{1}{2} \|\vec{S}_l\|^2$ so that solutions remain on the correct manifold. This is generally not the case for a classical integrator with equation (2), though it is for the system given by (3) and (4).

If the Hamiltonian (1) is split as $H = H_x + H_y + H_\lambda = (-J S_{1x} S_{2x}) + (-J S_{1y} S_{2y}) + \lambda(S_{1x} + S_{2x})$, with corresponding induced vector fields $X_H = X_{H_x} + X_{H_y} + X_{H_\lambda}$, then the solutions to the individual components of the vector field are given respectively by rotations $R_x(t)$ and $R_y(t)$ about the x and y axes due to the interaction between the two spins and a rotation $R_\lambda(t)$ about the x axis due to the interaction between the spins and the applied magnetic field. The angles of rotation for the x, y and λ components are $\alpha_l = t J S_{mx}(t_0)$, $\beta_l = t J S_{my}(t_0)$ and $\gamma = -t\lambda$, respectively. Replacing t with a time step τ and composing the rotations gives a symplectic integrator for the system (2). An integrator of order N is then given by choosing $a_i, b_i, c_i, \ i = 1, \ldots, k$ such that $\vec{S}(t_0 + \tau) = \prod_{i=1}^{k} R_x(a_i \tau) R_y(b_i \tau) R_\lambda(c_i \tau) \vec{S}(t_0) + \mathcal{O}(\tau^{N+1})$.

We use the second-order method given by $k = 6$ and $a_1 = b_2 = c_3 = c_4 = b_5 = a_6 = \frac{1}{2}$ with all other a, b, c set to zero. This is the well-known 'generalized leapfrog' method. The central stages of the method coalesce and can be combined, also, when output is not required at every step the outer stages of the composition can also be combined so that the method requires only four stages per time-step.

More details on the derivation of splitting methods for geometric integration, in particular, higher-order splittings with a minimal number of stages, can be found in [13]. The choice of optimal coefficients for such splittings is discussed in [10].

Poincaré surfaces of section (PSSs) can give a view of the general dynamical properties of a system; in particular, they can show the existence of chaotic orbits. Here we show PSSs for $\lambda = 0.2$ and 2.5. (PSSs for $\lambda = 0.02, 0.2, 0.5$ and 2.5 are shown in [14].) Trajectories for the PSSs were calculated by using the generalized leapfrog method to integrate the system (2) (with a step size of 0.1). The sections were taken with $\theta_2 = \pi/2$ and $\dot{\theta}_2 > 0$, i.e. $S_{2z} = 0$, $\dot{S}_{2z} < 0$, and at energy $E = -0.1$. The domain of the section is therefore a region on the unit sphere corresponding to the first spin. We use this section for consistency with [1], although we will show below that it is not in fact well-defined, leading to puzzling phase portraits.

The resulting PSSs are shown in figure 1 where they are compared with PSSs generated using equations (3) and (4) with a black-box classical integrator (in this case ode45 with RelTol $= 10^{-4}$, an order (4,5) Dormand–Prince pair with step size control from the package *odesuite*; see [15] for details). The computation times for the orbits using the ode45 integrator were about ten times longer than those for the same orbits calculated with the generalized leapfrog integrator.

The PSSs produced by the two different integrators show the same chaotic regions appearing for the same values of λ. The PSSs also qualitatively match those in [1]. The 'smearing' of the invariant curves of the PSSs from the classical integrator is due to orbits moving away from the constant energy manifold, especially near the singularity when spherical coordinates are used. The integration times for the orbits are therefore limited for this integrator.

The similarities between the results from the leapfrog method and the black-box method in figure 1 indicate that the curious 'folding' behaviour at the top and bottom of the PSSs ($\theta = 0 \mod \pi$) is due to the equations of motion rather than being an effect of the coordinate singularity in equation (3), as is claimed in [1].

A more natural approach to the PSSs is to plot the points on the surface of the unit sphere which prevents the regions about $\theta_1 = 0$ and $\theta_1 = \pi$ from being distorted. Figure 2 shows the resulting view of the PSSs for the generalized leapfrog method.

Not all of the points on the sphere S_1 correspond to an initial condition for a point on the PSS. For fixed energy E, the excluded region is bounded by a closed curve on the unit sphere; namely, for $S_{1x} \in [-1, 1]$,

$$S_{1y}^2 < \frac{(E - \lambda S_{1x})^2 - (J S_{1x} - \lambda)^2}{J^2}, \qquad S_{1z}^2 = 1 - S_{1x}^2 - S_{1y}^2. \qquad (5)$$

Figure 3 shows the excluded regions of the PSSs for $E = -0.1$ and $\lambda = 0.2$ and 2.5. When λ is small the excluded regions include the north and south poles of the spheres. For large values of λ, the excluded region also becomes large and its centre shifts towards the equatorial plane.

The flow of the system is tangential to the PSS (i.e. $\dot{S}_{2z} = 0$) along the boundaries of the excluded regions. The Poincaré map can become singular along these curves which explains the apparently singular behaviour of some of the invariant curves in figure 3.
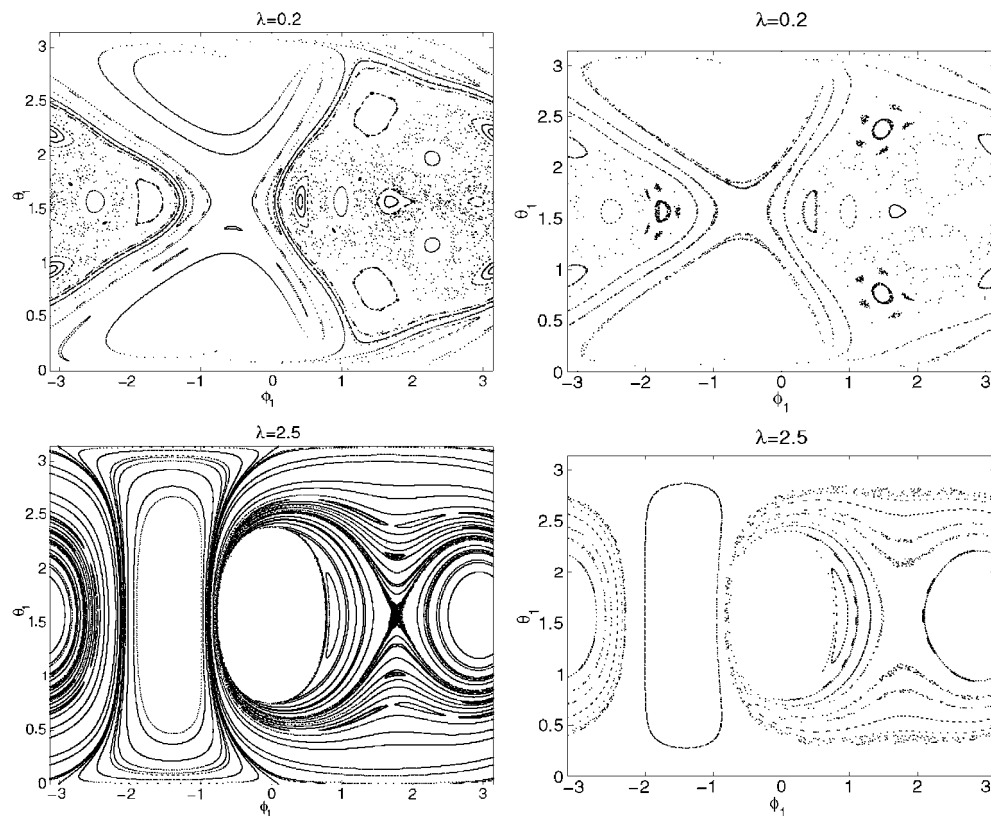
Figure 1. Poincaré surfaces of section in spherical polar coordinates ($\rho = 1$), on the sphere corresponding to $\vec{S}_1$, for $\lambda = 0.2$ and 2.5 with energy $E = -0.1$, generated with the generalized leapfrog method with $\tau = 0.1$ (left) and with a black-box classical integrator `ode45` with `RelTol` $= 10^{-4}$ (right). Typical orbit lengths are $(1 \sim 100)(100\pi)$ for the leapfrog orbits and $(1 \sim 3)(100\pi)$ for `ode45`. An orbit of length 100π corresponds to about 125 crossings of the section.

The singularity in the equations of motion for the spherical coordinates can lead to large local errors from numerical integrators when the solution passes close to the singularity. However, large errors in the coordinates need not lead to large errors in position. To explore this question we calculated the Euclidean error in the position, after a single time-step, for decreasing values of θ_1, using the generalized leapfrog (LF) method in Cartesian coordinates and the second-order Runge–Kutta (RK2) method with the equations of motion in spherical coordinates. Choosing ϕ_2 and θ_2 away from a singularity, the L_2 error in $\vec{S}$ was calculated for a range of values of ϕ_1, θ_1 and λ. Taking the worst case over the range of ϕ_1 values showed that for values of θ_1 away from 0 and π, local errors in the LF and RK2 methods are similar (figure 4). However, as $\theta_1 \rightarrow 0$ the local error for RK2 grows as $\mathcal{O}(\theta_1^{-2})$ while the error for LF remains constant.

Energy conservation can give a second indication of the effect of the coordinate singularity. A trajectory passing within about 0.1 of a singularity is sufficient to cause a jump in E of 100% with RK2. Trajectories passing closer to the singularity cause larger jumps. The singularity due to the choice of coordinate system has a far larger effect on the energy error than the choice of integrator: the same calculation performed with RK2, but in Cartesian

λ=0.2 λ=2.5
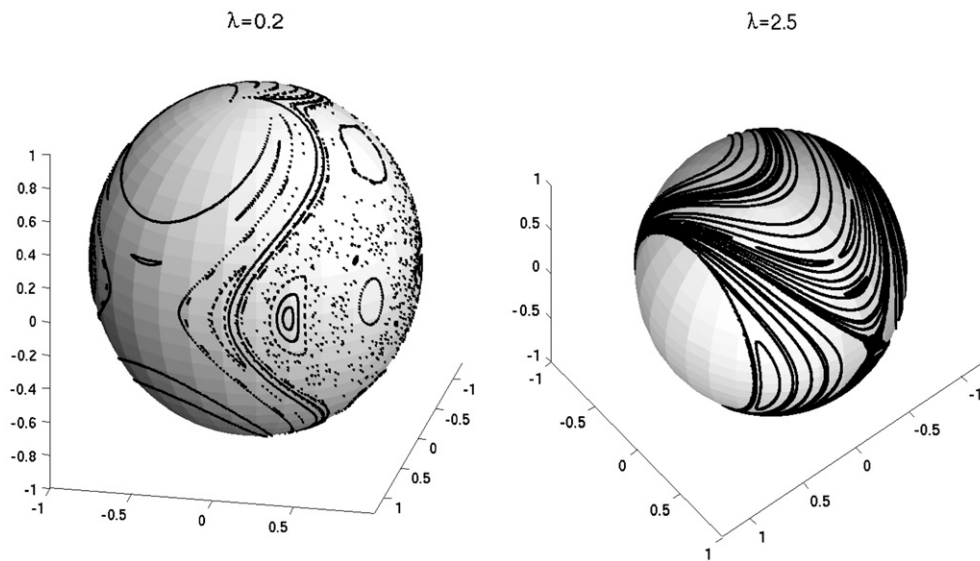
Figure 2. Poincaré surfaces of section, in Cartesian coordinates, for λ = 0.2 and 2.5 with energy $E = -0.1$ generated with the generalized leapfrog method when plotted in spherical coordinates.
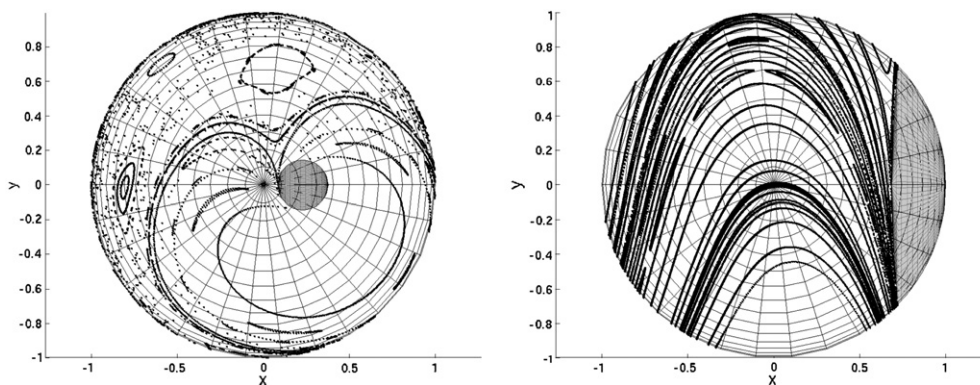
Figure 3. PSSs in Cartesian coordinates for $E = -0.1$ and λ = 0.2 and 2.5 as viewed from the north pole of the sphere. The excluded regions are shaded.

(non-singular) coordinates showed a drift in the energy of about 2.5% per 5000 time-steps (for $\tau = 0.1$). In comparison, the energy of the same solution calculated with the leapfrog integrator oscillated about the initial energy in a regular fashion and with a maximum amplitude for the oscillations of about 2.5% of the total energy.

In conclusion, it is necessary to pay attention to both the integration method and the coordinate system used in order to accurately calculate orbits of the two-spin system numerically. Appropriately chosen geometric numerical integration methods are able to offer vastly superior results for spin systems. Also, when calculating PSSs it is necessary to give consideration to the topology and domain of the section. Naively chosen sections can easily
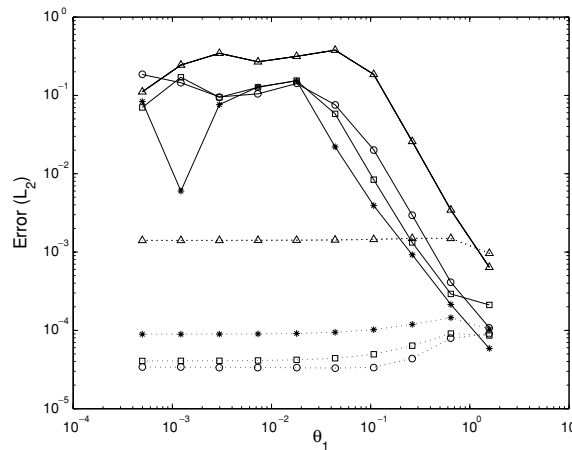
Figure 4. Local error (with $\tau = 0.1$) as a function of θ_1 for the RK2 integrator with the equations of motion given in spherical coordinates (solid lines). Initial conditions: $\phi_2 = \pi/4$, $\theta_2 = \pi/2$ with ϕ_1 chosen so as to give an approximate 'worst-case' for the local error. The local errors for the leapfrog integrator (and equations of motion in Cartesian coordinates) are given for the same values of ϕ_2 and θ_2 as used for the RK2 results but with the value of ϕ_1 picked to give the 'worst' solution for the leapfrog integrator (dotted lines). Four values of λ were used: 0.02, 0.2, 0.5 and 2.5 (circles, boxes, stars and triangles, respectively). As θ_1 approaches zero the local error for the system in spherical coordinates grows like $\mathcal{O}(\theta_1^{-2})$.

fail to yield well-defined Poincaré sections, leading to singularities in the computed Poincaré maps.

References

[1] Robb D T and Reichl L E 1998 *Phys. Rev.* E **57** 2458–9
[2] Ree S and Reichl L E 1999 *Phys. Rev.* E **60** 1607–15
[3] Emerson J and Ballentine L E 2001 *Phys. Rev.* A **63** 052103
[4] Frank J, Huang W and Leimkuhler B 1997 *J. Comput. Phys.* **133** 160–72
[5] Steinigeweg R and Schmidt H-J 2005 *Preprint* math-ph/0504009
[6] Steinigeweg R and Schmidt H-J 2006 *Comput. Phys. Commun.* **174** 853–61
[7] McLachlan R I 1993 *Phys. Rev. Lett.* **71** 3043–6
[8] Reich S 1993 *Technical Report* 93-20 The University of British Columbia
[9] Marsden J E and Ratiu T S 1994 *Introduction to Mechanics and Symmetry* (New York: Springer)
[10] McLachlan R I and Quispel G R W 2002 *Acta Numer.* **11** 341–434
[11] Hairer E, Lubich C and Wanner G 2002 *Geometric Numerical Integration* (Berlin: Springer)
[12] Dullweber A, Leimkuhler B and McLachlan R I 1997 *J. Chem. Phys.* **107** 5840–51
[13] Yoshida H 1990 *Phys. Lett.* A **150** 262–8
[14] McLachlan R I and O'Neale D R J 2005 *Reports in Mathematics* 14 Massey University
[15] Shampine L F and Reichelt M W 1997 *SIAM J. Sci. Comput.* **18** 1–22